Rayanne Pinto Costa[1]
Department of Mechanical Engineering,
The University of Akron,
Akron, OH 44325
e-mail: rp98@uakron.edu

Blaise Simplice Talla Nwotchouang
Department of Biomedical Engineering,
The University of Akron,
Akron, OH 44325
e-mail: bn23@uakron.edu

Junyao Yao
Department of Mechanical Engineering,
The University of Akron,
Akron, OH 44325
e-mail: 695974649@qq.com

Dipankar Biswas
Department of Neurosurgery,
Johns Hopkins Medical Institutions,
Baltimore, MD 21205
e-mail: dbiswas6@jhmi.edu

David Casey
Department of Mechanical Engineering,
The University of Akron,
Akron, OH 44325
e-mail: david.m.casey88@gmail.com

Ruel McKenzie
School of Polymer Science and
Polymer Engineering,
The University of Akron,
Akron, OH 44325
e-mail: rmckenzie@uakron.edu

Frederick Sebastian
Department of Bioengineering,
Northeastern University,
Boston, MA 02115
e-mail: sebastian.f@northeastern.edu

Rouzbeh Amini
Department of Bioengineering,
Northeastern University,
Boston, MA 02115;
Department of Mechanical and
Industrial Engineering,
Northeastern University,
Boston, MA 02115
e-mail: r.amini@northeastern.edu

David A. Steinman
Department of Mechanical & Industrial
Engineering,
University of Toronto,
Toronto, ON M5S 3G8, Canada
e-mail: steinman@mie.utoronto.ca

Impact of Blood Rheology on Transition to Turbulence and Wall Vibration Downstream of a Stenosis

Previous experimental flow studies have demonstrated a delay (∼20%) in transition to turbulence for whole blood compared to a Newtonian analog fluid in both a straight pipe and eccentric stenosis model with ridged walls. The impact of wall compliance on the transition to turbulence of blood compared to Newtonian analog and on wall vibration is unknown. The present study employed flexible walls downstream of an eccentric stenosis model and examined the wall vibration during the transition to turbulence with whole blood and a Newtonian analog. Measurements of tube wall vibration velocity (WVV) were used as an indicator of the turbulence level within the flexible tube. WVV was measured at 5, 10, and 15 diameters downstream of the stenosis using a laser Doppler vibrometer at Reynolds numbers 0, 200, 300, 350, 400, 450, 500, 550, 600, 650, 700, and 750. The root mean squares (RMS) of the measured WVV were utilized as an indirect measure of fluid velocity fluctuations present at that location, and hence, an indicator of transition to turbulence. WVV RMS was near-constant until approximately Reynolds number 400. It increased monotonically with Reynolds number for both whole blood and the Newtonian fluid. No differences in the transition to turbulence were observed between whole blood and the Newtonian fluid, as the WVV RMS curves were remarkably similar in shape. This result suggests that rheology had minimal impact on the WVV downstream of a stenosis for transition to turbulence since the fluids had a similar level of vibration.
[DOI: 10.1115/1.4055856]

Keywords: transition, turbulence, blood, laser Doppler vibrometer, non-Newtonian, rheology, fluid dynamics

[1]Corresponding author.
Manuscript received November 17, 2021; final manuscript received September 27, 2022; published online December 5, 2022. Assoc. Editor: Sarah Vigmostad.

Francis Loth
Department of Bioengineering,
Northeastern University,
Boston, MA 02115;
Department of Mechanical and Industrial
Engineering,
Northeastern University,
Boston, MA 02115
e-mail: f.loth@northeastern.edu

Introduction

Blood is a non-Newtonian fluid composed of a complex mixture of cellular elements (red blood cells (RBCs), white blood cells, and platelets) suspended in a nutrient-rich aqueous solution (plasma).The shear-thinning properties of blood are dependent on the characteristics of its components, such as red blood cell aggregations, the deformability of RBCs, viscosity of plasma, and hematocrit [1]. At lower shear stresses, RBC tends to aggregate and disperse as shear stress increases. The aggregation results in a higher viscosity. The deformability of RBCs can also affect viscosity. The loss of deformability increases viscosity [2]. Blood is known to have a near-Newtonian behavior at high shear rates above $200\,s^{-1}$ [3]. Several studies have examined the flow field downstream of a rigid axisymmetric stenosis using a Newtonian fluid [4,5]. However, less is known about the impact of the non-Newtonian nature of blood on the transition to turbulence. Some recent studies have revealed blood transitions to turbulence at a slightly higher Reynolds number than a Newtonian fluid analog experimentally and numerically [3,6]. Biswas et al. compared the transition to turbulence between whole porcine blood and water–glycerin (WG) mixture experimentally in a rigid straight pipe using a Doppler ultrasound probe to measure fluid velocities [3]. The flow was steady, and the Reynolds number was based on measured viscosity at a shear rate of $1000\,s^{-1}$. The authors used two mathematically defined markers to determine the critical Reynolds number (Recr). One marker was based on the turbulent kinetic energy (TKE) and showed that blood transitions on average at $Re_{cr} = 2806 \pm 109$ while water–glycerin at $Re_{cr} = 2316 \pm 34$. The Reynolds number was delayed by approximately 21% in blood compared to water–glycerin. The second marker was based on the velocity profile change, which showed that blood transitions on average at $Re_{cr} = 2871 \pm 104$ while water–glycerin at $Re_{cr} = 2403 \pm 8$. Costa et al. conducted a similar study using a Doppler ultrasound probe downstream of a 5% eccentric stenosis (area restriction of 75%) in a rigid flow system [7]. The Reynolds numbers were also based on the viscosity measured at a shear rate of $1000\,s^{-1}$. The velocities were measured 12 diameters downstream of the throat of the stenosis. Using TKE, they found that whole blood transitioned at $Re_{cr} = 470 \pm 27.5$ and water–glycerin at $Re_{cr} = 395 \pm 10$ ($\sim$19% delay). Transition to turbulence in blood has also been studied numerically. Khan et al. used the same nonaxisymmetric stenosed rigid geometry as Varghese et al. and Costa et al. to investigate the stabilizing effect of the shear-thinning fluids [6]. A shear-thinning model was used based on a curve-fitting of experimental blood data from Biswas et al. Similar to Biswas et al. and Costa et al., Khan et al. also found a delay in the transition to turbulence of blood compared to a Newtonian fluid. The shear-thinning model showed transition at $Re_{cr} = 760$ and the Newtonian model at $Re_{cr} = 700$ using infinite–shear viscosity.

The above-cited studies all employed rigid walls, and it is unclear how wall compliance might affect fluid instabilities in the transition to turbulence downstream of a stenosis. For example, wall-compliant coatings have been studied as a passive method to delay the transition to turbulence and reduce skin-friction drag at a high Reynolds number. However, there is controversy as to the efficacy of this approach [8]. More specifically, it is unknown if the differences observed for transition to turbulence between whole blood and a Newtonian analog fluid in rigid pipes [3,7] will also be present for a compliant tube, given that the fluid–structure interaction may have an impact on flow dynamics and blood being a particulate fluid. Experimental studies have shown evidence of wall vibration being induced by turbulence [9–12]. Those studies were in vivo and focused on understanding the relationship between graft failure and turbulence. Loth et al. and Lee et al. investigated the transitional flow in a venous anastomosis arteriovenous graft in vivo and numerically [9,10]. The flow in an arteriovenous graft creates high wall shear stress, flow separation, and pressure fluctuations similar to the flow downstream of an arterial stenosis [9]. The wall vibration velocity measurement (WVV) was conducted using a laser Doppler vibrometer (LDV). Those numerical simulations demonstrated an increase in the velocity and pressure fluctuations in the same graft location as the elevated WVV [9]. Another study that shows evidence of flow-inducing WVV was done by Fillinger et al. [11]. They used color Doppler ultrasound to measure tissue vibration surrounding the blood vessel. The results suggested that the tissue vibration observed was a result of the kinetic energy transfer from the vessel wall due to flow disturbance at elevated Reynolds numbers. Kirkeeide et al. also investigated the wall vibration induced in vivo and in vitro but in an axisymmetric stenosis under steady flow [12]. Wall displacement measurements were conducted with a piezo-electric crystal contact microphone. The vibrational signal intensity at downstream positions showed an increase in wall vibration to a maximum, and then, it decayed to a near-constant level. At the position where the great vibration occurred, the amplitude of wall vibration increased with stenosis area reduction or an increase in Reynolds number. The location of maximum vibration downstream the stenosis was believed to coincide with the jet reattachment point.

Based on the close association of WVV and turbulence described previously [9,10,12], the present study utilized a measurement of WVV to compare the transition to turbulence between whole blood and a Newtonian fluid in a compliant tube downstream of an eccentric stenosis. The study aimed to determine the impact of a flexible tube downstream of an eccentric stenosis in transition to turbulence for whole blood compared to a Newtonian analog fluid. More specifically, this study aimed to verify if the presence of wall compliance impacts the delay in transition to turbulence of blood versus a Newtonian fluid compared to the delay observed previously in a rigid pipe model of the same stenosis geometry.

Methods

Experimental Setup. The experiment consisted of measuring fluid rheology and density, flowrate, temperature, and compliant wall velocity. The wall velocity measurements were conducted

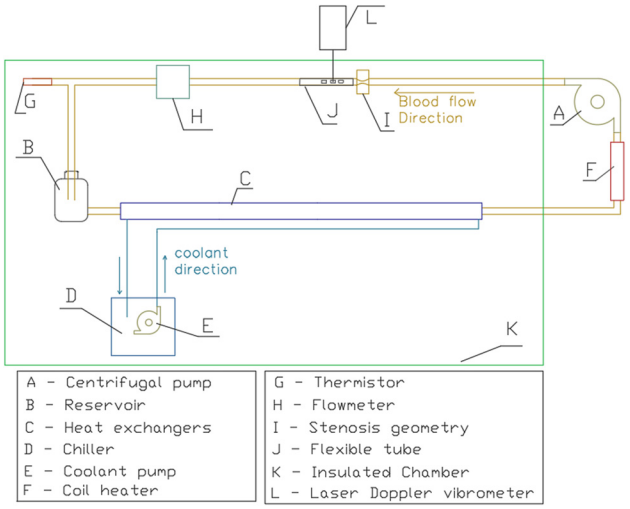

Fig. 1 Experimental setup

inside an automated flow circuit similar to the one described previously by Biswas et al. [3] and Costa et al. [7]. The geometry analyzed was a 5% eccentric stenosis with 75% area reduction in the throat, which is the same geometry as Costa et al. [7]. The inner diameter upstream and downstream of the stenosis was 6.35 mm. The 75% area reduction and 5% eccentricity in the stenosis geometry was achieved by the subtractive machining of a $^1/_2$-in.-thick solid Delrin® acetal resin bar (McMaster Carr, Elmhurst, IL). Acetal resin was chosen because of its ability to resist expansion due to heat and moisture; thus, it can be machined to close tolerances. The opening was machined from each end up to the throat, starting with a solid bar with a tolerance of 25 μm. The material was then machined from the outside at each end such that a 0.25-in. (6.35 mm) acrylic pipe would fit snugly at each end. The stenosis had outside dimensions of 0.5 in. × 1.25 in. × 1 in (12.7 mm × 31.75 mm × 25.4 mm).

The flow system for the test setup is shown in Fig. 1. The system is composed of a Sarns 7850 disposable centrifugal pump (A in Fig. 1) that drives the test fluid (water–glycerin or blood) from the reservoir (B) through an eccentric stenosis geometry in a closed-loop (I). The temperature of the test fluid is controlled using a coolant pump (E) and a heater coil (F). The pumps and heater coil are powered by switching DC power supplies (BK Precision 1685B, Yorba Linda, CA). The cooling system is composed of a Neslab RTE-110 chiller (D), which chills the coolant to 27 °C, along with four glass heat exchangers (C). An immersion thermistor probe (±0.15 °C, CDP25-TH-A & OL-703, OMEGA Engineering, Inc., Stamford, CT; indicated as G in Fig. 1), and a transit time ultrasonic flowmeter (±0.5 °C, a TS410 flowmeter with ME6 PXN sensors; Transonic Systems Inc., Ithaca, NY; indicated as H in Fig. 1) was used to monitor the temperature and flowrate.

A straight acrylic pipe was placed between the centrifugal pump and the stenosis. This entrance pipe had a diameter of 6.35 mm and a length of 0.65 m. This length is longer than the laminar entrance length needed for a Reynolds number of 750 (the largest Reynolds number examined), ensuring the flow would be fully developed when entering the stenosis. A turbulator mixer was placed at the exit of the pump and consisted of a plastic fishing line in an X-shape across the acrylic pipe. The turbulator was inserted downstream of the pump to help provide consistent flow conditions. A piece of 15 mm acrylic tube was also used to connect the stenosis to the latex tube of length 130 mm (McMaster-Carr, Elmhurst, IL; indicated as J in Fig. 1), inner diameter 6.35 mm, and outer diameter 7.94 mm. An LDV (model OFV-534, Polytec Holding AG, Hörsching, Austria; indicated as L in Fig. 1) was used to measure the wall velocity of the latex tube downstream of the stenosis. The LDV laser beam passed through a hole in the insulated chamber. The wall vibration measurement was conducted at three locations downstream of the stenosis: 5D, 10D, and 15D (D-diameter) in the latex tube (See Fig. 2). In these positions, squared pieces of Polytec A-RET-T010 reflective tape (Polytec, Inc., Dexter, MI; indicated in Fig. 2) were used to help reflect the beam. The laser Doppler vibrometer was mounted on a tripod (3251 Manfrotto, Bogen, Italy). The tripod allowed the operator to perform a manual lateral change of positions while at the same height. The latex tube wall velocity measurements were conducted at Reynolds numbers 0, 200, 300, 350, 400, 450, 500, 550, 600, 650, 700, and 750. At each location, the following data were acquired for 3 s at a sampling rate of 250 kHz using a NI USB-6259 data acquisition device (National Instruments, Austin, TX): wall velocity (from LDV), temperature (from the thermistor), and flowrate (from the flowmeter). Data points were repeated if the required limits for temperature (36.5–37.5 °C), and Reynolds number (±1.5%) were exceeded. The elastic properties of the latex tube (0.25″ ID, 5/16″ OD. McMaster-Carr, Super-soft rubber tubing for air and water, Part No. 5234K98, hardness value 40 A) were evaluated experimentally using a micro-indenter (Biomomentum Inc., Laval, QC, Canada, Model: Mach-1 v500c). Results were obtained on one sample at three different locations at 37(±0.1) ° C and repeated five times at each location. Each indentation was 0.2 mm at a speed of 0.030 mm/s. Elastic modulus was computed using the methodology for an indenter as described by Whitcomb et al. [13] and Hayes et al. [14] with a Poisson ratio of 0.5, latex material thickness of 0.794 mm, a flat-cylindrical indenter with radius of 0.5 mm, and Hayes correction factor 2.3076. The material displayed a linear elastic response ($r^2 = 0.999$, $p < 10^{-9}$, slope = 3381 mN/mm). The mean and standard deviation of the elastic modulus at the three locations was 1.103 (±0.016), 1.097 (±0 .010), and 1.091 (±0.011) MPa. The average over all locations was 1.097 (±0.005) MPa.

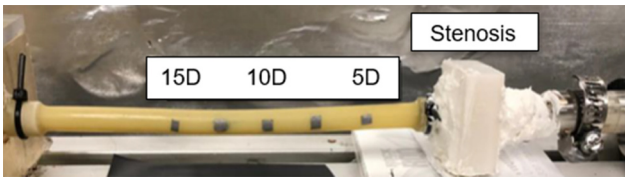

Fig. 2 Photograph of compliant section with LDV measurement locations indicated. Flow direction is right to left.

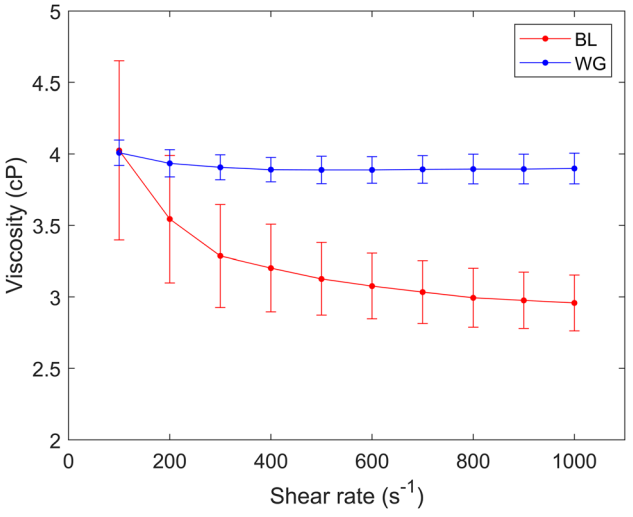

Fig. 3 Mean viscosity measurements of blood (BL) and water–glycerin (WG) samples at several shear rates (100–1000 s^{-1}). Error bars are SD. The reference viscosity was at the shear rate of 1000 s^{-1}.

Table 1 Viscosity at 1000 s^{-1} and density before the experiments for blood and water–glycerin

	Blood						
Test #	1	2	3	4	5	Mean	SD
Viscosity (cP)	2.75	2.79	3.19	3.03	3.06	2.94	0.17
Density (g/ml)	1.07	1.09	1.08	1.05	1.04	1.07	0.018
	Water–glycerin						
Test #	1	2	3	4	5	Mean	SD
Viscosity (cP)	3.73	3.91	3.91	3.91	4.03	3.90	0.10
Density (g/ml)	1.13	1.13	1.12	1.16	1.12	1.13	0.01

Torsional Rheometry. The fluid viscosity was measured using AR200 EX parallel plate rheometer (AR2000ex, TA Instruments Inc., New Castle, DE). The geometry used was a 60 mm diameter steel parallel plate in a 500 μm gap. The Peltier plate was at 37 °C. The rotational speed was held constant for 25 s, but the data were acquired for 5 s. The viscosity was measured at the shear rates 100, 200, 300, 400, 500, 600, 700, 800, 900, and 1000 s^{-1}. Calibration of the rheometer was checked using Cannon S3 standard fluid at a temperature of 37.78 °C. The system was recalibrated at the start of the measurement day so that the error would be less than 3%. The viscosity measured at a shear rate 1000 s^{-1} for blood and water–glycerin was used to calculate the Reynolds number.

Experimental Procedure. The Newtonian blood analog was a water–glycerin (52:48% by volume) mixture. Anticoagulant (3.8 g sodium citrate in 100 ml distilled water) was mixed into each 900-ml aliquot of blood to reduce clotting during the experiment. The blood was purchased from a slaughterhouse (3D Meats, Dalton, OH) and preheated to 37 °C before loading into the flow system. Once loaded into the system, the flowmeter was calibrated using a stopwatch and a graduated cylinder. The viscosity was measured at 10 different shear rates: 100, 200, 300, 400, 500, 600, 700, 800, 900, 1000 s^{-1}. The viscosity at a shear rate of 1000 s^{-1} was used as the reference viscosity for calculating the Reynolds number. Density was measured using a 250-ml graduated cylinder and a high-resolution scale (PB1502, Mettler Toledo, Columbus, OH). The flow rates for the experiments were adjusted to realize a total of 11 Reynolds numbers ranging from 200 to 750 based on the density and viscosity measured prior to the experiment. All pipes and tubing were cleaned after each experiment by flushing with a water-Alconox mixture, followed by a one-hour rinse with tap water; the pipes and tubing were subsequently dried using compressed air. A total of five separate studies were conducted since one sample might be prone to variability and to be consistent with previous studies [7].

Wall vibration velocity on the latex tube was acquired at positions 5D, 10D, and 15D using LDV. All Reynolds numbers were acquired at each location before moving to the next position. The WVV amplitude spectrum (AS) was calculated by multiplying the fast Fourier transform by its complex conjugate and then taking the square root [9]. The average WVV AS was then obtained by averaging the five tests together to obtain average amplitude

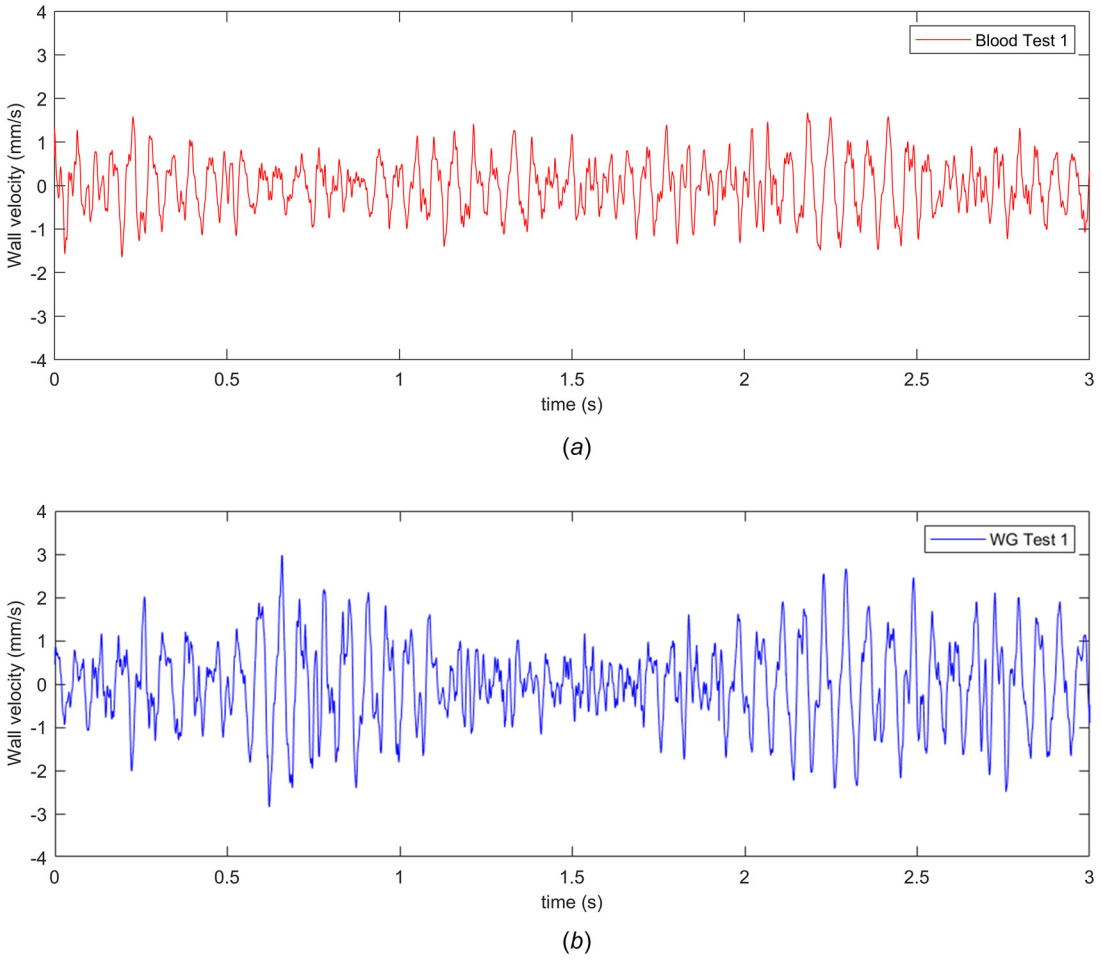

Fig. 4 Wall vibration velocity (WVV) time trace of Test 1 for blood (*a*) and water–glycerin (WG) (*b*) at Reynolds number 750 and position 15D

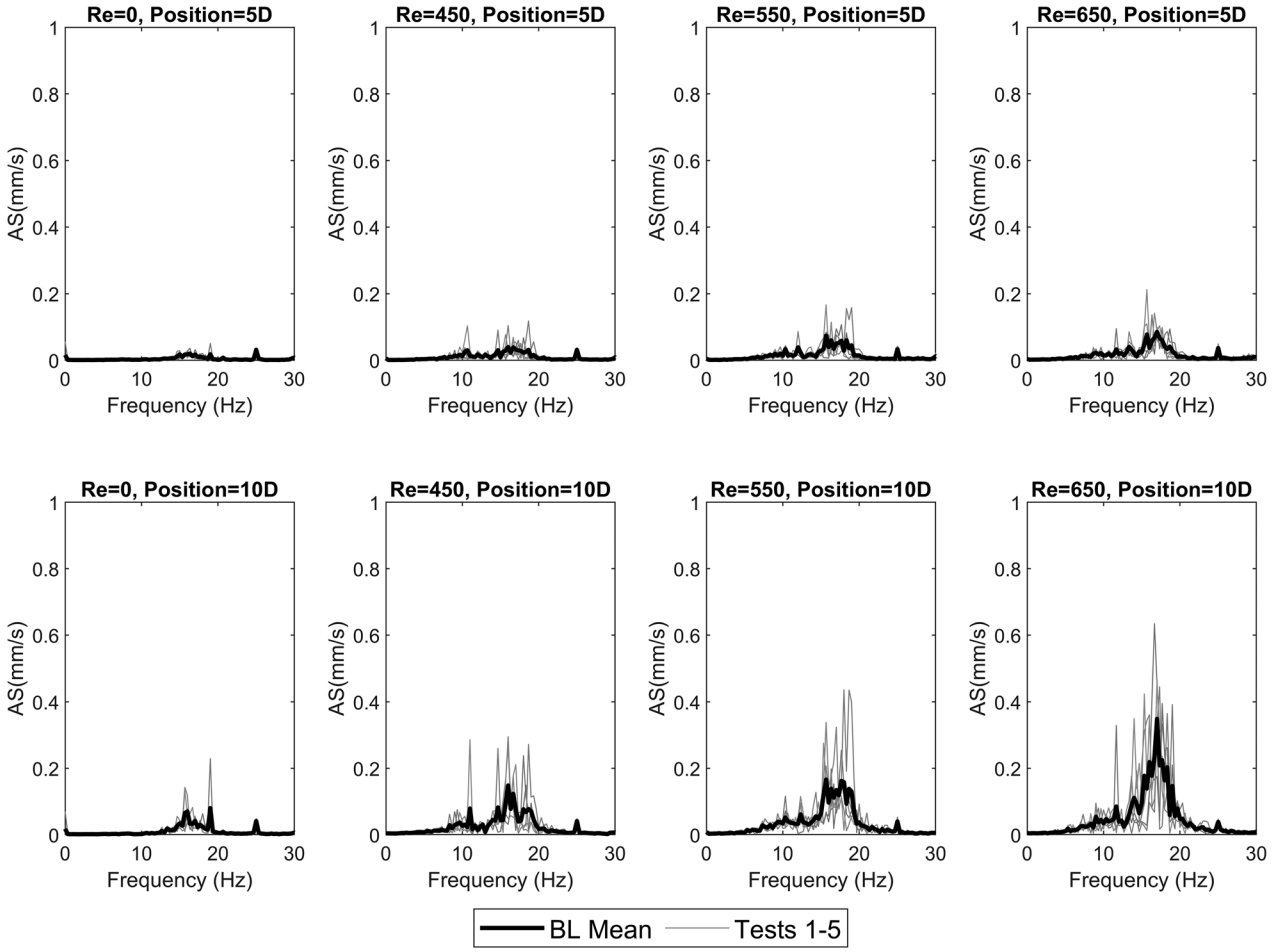

Fig. 5 Wall vibration velocity (WVV) amplitude spectrum (AS) of the five samples in gray line and mean in black line for blood (BL)

versus frequency. The root-mean-square (RMS) of WVV time trace was also computed after the application of a low-pass filter to remove frequencies above 200 Hz. To minimize spurious noise, we applied a filter at a frequency approximately one order of magnitude larger than the WVV frequencies of interest (200 Hz).

The standard deviation (SD) of the five tests was also calculated. The natural frequency of this specific tube-stenosis geometry was obtained by a standard bump test. This bump test was conducted three times with the system filled with water–glycerin with the pump turned off (i.e., $\mathrm{Re} = 0$). A tap with a wooden ruler was made on the tubing on position 10D, and WVV was recorded at the same location.

Results

Rheology. Figure 3 presents the mean viscosity of blood and water–glycerin averaged over the five samples as a function of the shear rate measured before each experiment. The water–glycerin viscosity was constant with shear rate, and the whole blood exhibited a weakly shear-thinning behavior as expected. At $1000\,\mathrm{s}^{-1}$, the average viscosity for water–glycerin and blood was 3.90 cP and 2.94 cP, respectively. The measured density at 37 °C and the viscosity at $1000\,\mathrm{s}^{-1}$ for each sample are shown in Table 1.

Wall Vibration Velocity. An example of WVV trace of the tube wall downstream of the stenosis for blood and water–glycerin at position 15D and Reynolds number 750 is shown in Fig. 4. This figure demonstrates that fluid velocity fluctuations are detectible on the wall surface of the flexible tube by the LDV system. The average AS of the five samples and SD for blood and water–glycerin in position 5D and 10D at Reynolds numbers 0, 450, 550 and 650 are shown in Figs. 5 and 6, showing the dominant frequencies ranging between 15 and 19 Hz. The bump-test revealed that the natural frequency for the system was exactly 17.284 Hz for all three tests, which is near the value observed for both laminar and transitional Reynolds numbers as well as the $\mathrm{Re} = 0$ condition (pump off) in this geometry. The average WVV RMS of the five experiments comparing blood and water–glycerin are shown in Fig. 7, showing the trend with Reynolds number with a visually obvious inflection point near Reynolds number 400. For comparison, Fig. 8 shows the ratio of average WVV RMS of blood to water–glycerin over the five tests at all Reynolds numbers and each location. The average of the ratio of WVV RMS for blood to water–glycerin for over all Reynolds numbers was 0.95, 0.90, and 0.86 for positions 5D, 10D, and 15D, respectively.

Discussion

The results show that whole blood had a similar WVV RMS as the Newtonian analog fluid during the transition to turbulence (i.e., no detectable delay) under steady flow within a flexible tube downstream of a 5% eccentric stenosis with a 75% area reduction (Fig. 7). This is in contrast to the ∼19% delay in transition to turbulence observed in the rigid pipe model with the same geometry [7]. This could be due to alteration in the flow dynamics caused by fluid–structure interaction or because the WVV measurement technique is not sensitive enough to observe differences in fluid velocity fluctuations. Blood and water–glycerin had a similar

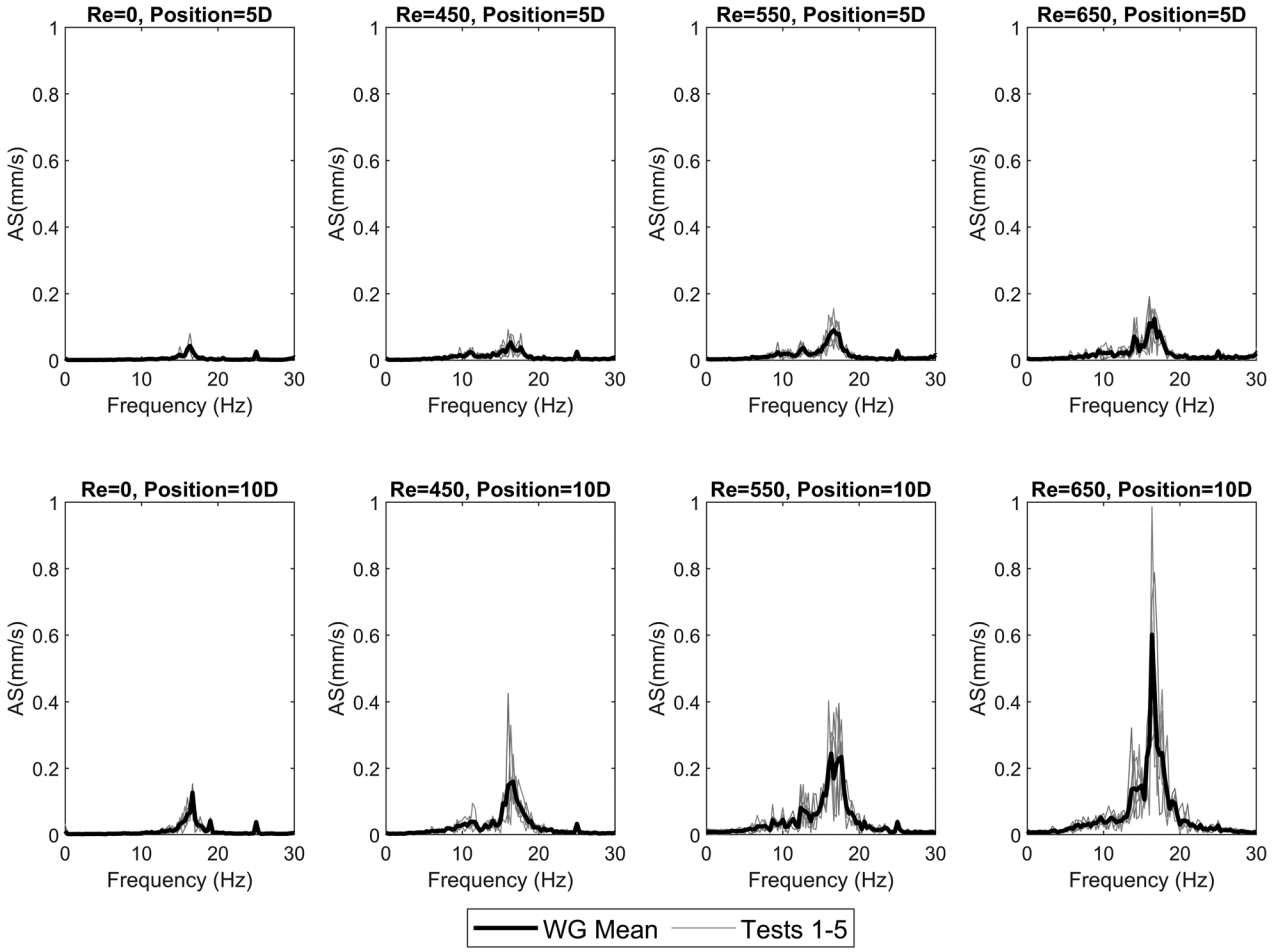

Fig. 6 Wall vibration velocity (WVV) amplitude spectrum (AS) of the five samples in gray line and mean in black line for water–glycerin (WG)

curve shape for each measurement location (Fig. 7). Their curves rise gradually, with an inflection point occurring approximately near Reynolds number 400, which is near the Re_{cr} found by Costa et al. using a rigid wall stenosis model with the same geometry [7]. However, the study was able to identify a delay in the transition to turbulence by measuring the flow velocity fluctuations using a pulsated Doppler ultrasound probe with the rigid wall. The Re_{cr} for blood was 470 ± 27.5, which was 19% larger than water–glycerin with 395 ± 10. Numerical results from Khan et al. also found a delay which showed that Re_{cr} was 760 for blood (shear thinning model) and 700 for water–glycerin based on infinite shear viscosity. However, when using the definition of Reynolds number based on domain-averaged viscosity a posteriori found Re_{cr} to be 710. These Reynolds numbers are higher than those found in the present study [6], which may be due to noise inherent in the experiments that are not typically accounted for in simulations [15]. Kirkeeide et al. estimated that the wall vibrations could be discerned from the background noise for Reynolds number 600–620 for a 75% area reduction; however, these values were for axisymmetric stenosis [12]. Blood also had a slightly smaller average WVV RMS compared to water–glycerin. This could be a result of the viscoelasticity effects of blood, such as shear thinning or the density differences between the two fluids. Khan et al. found that the shear-thinning model presented a smaller volume-average TKE compared to the Newtonian fluid, which they expected since there was an increase in viscosity in regions of low shear rates (i.e., recirculation zone) [6]. However, their study did not account for other viscoelastic effects of blood, which according to the authors, can also play a role in the transition to turbulence by the dampening of turbulent intensities. Also, the present study might increase the residence time compared to in vivo since in an in vivo pulsatile condition it is more likely to have shorter residence times downstream of stenosis compared to an in vitro steady flow model. It would seem rather difficult to design an experiment that could discriminate between the shear-thinning and the other viscoelasticity effects; however, one could imagine an experiment that could identify the independent effect of density on WVV during the transition to turbulence.

Our results also revealed that position 5D had $\sim$1.7 – 2.5 times lower wall vibration compared to positions 10D and 15D. Positions 10D and 15D had similar amplitude. This variation is consistent with Khan et al. [6] and Varghese et al. [5], who showed TKE varied with position downstream of the stenosis. This is also consistent with previous arteriovenous graft studies [9–10] that demonstrated wall vibration is a local phenomenon and primarily confined to the region of turbulence. The position 5D may have lower WVV than the other locations due to smaller fluid velocity fluctuations, although it could also be related to proximity to the clamp location.

Note that the measurement of wall vibration is an indirect way to measure the level of turbulence in the flow and was chosen due to the structural sealing limitations that prevented the use of a Doppler ultrasound probe, which would require insertion into the flow field. WVV method may not have sufficient sensitivity to observe the delay in transition observed by Costa et al. [7]. Nevertheless, the results from our study show that rheology has minimal impact on the wall vibration during the transition to turbulence. The consistency of vibration frequencies indicates wall resonance phenomena, albeit at frequencies lower than would be seen for arterial tissue in vivo. Further research using a more direct

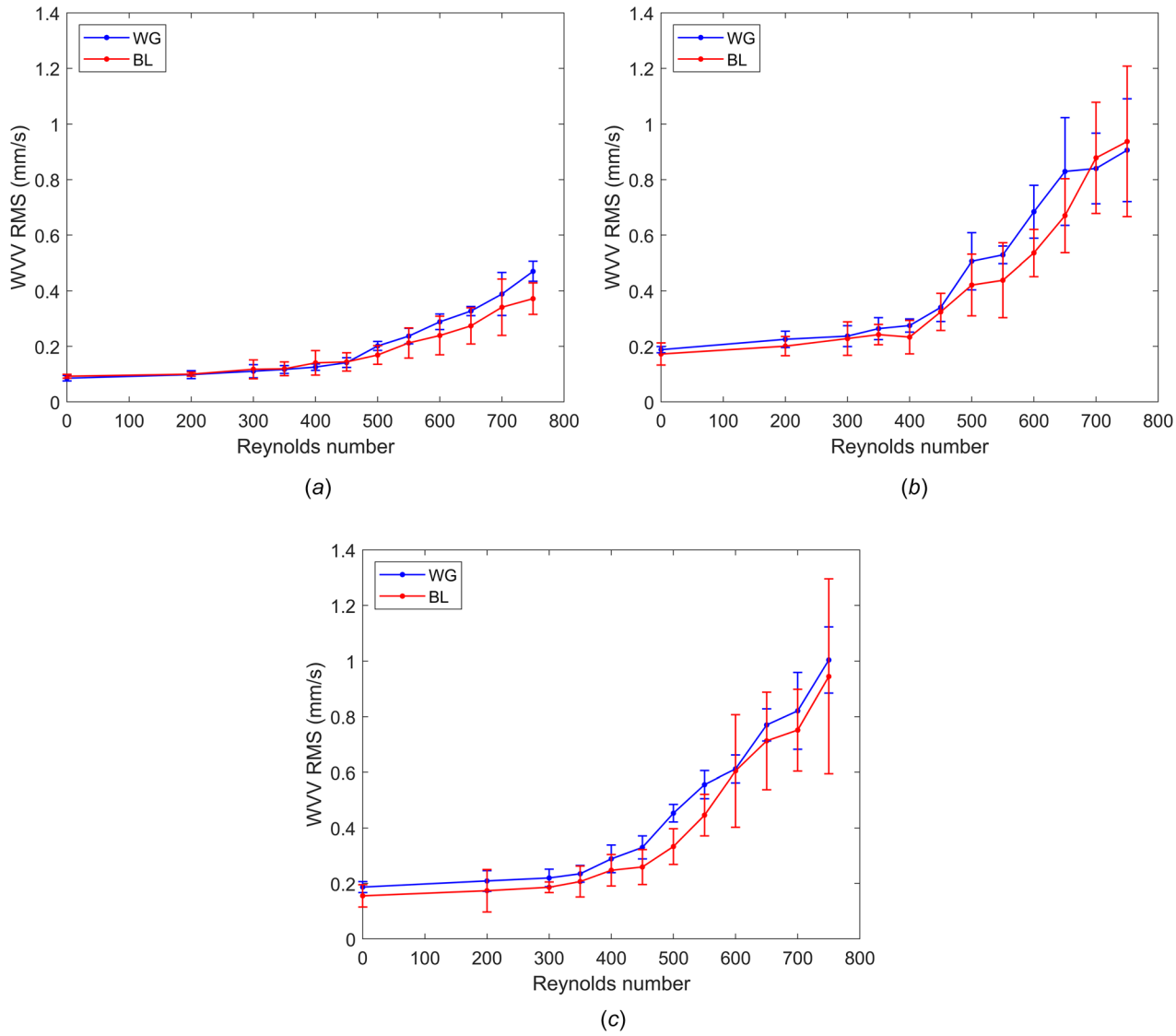

Fig. 7 Comparison of blood (BL) and water–glycerin (WG) average wall vibration velocity (WVV) RMS with error bar as SD: (*a*) 5D, (*b*) 10D, and (*c*) 15D

measurement of fluid velocity is required to fully understand the impact of a flexible wall on the transition to turbulence, even for simple fluids.

Finally, we note that the average of the ratio of WVV RMS for blood to WG over all Reynolds numbers was 0.95, 0.90, and 0.86 for positions 5D, 10D, and 15D, respectively (Fig. 8). In addition, distinct variations of this ratio with Reynolds number were observed at each of the three axial positions examined. The cause of this is unclear and hints at a possible difference in the behavior of blood versus WG, even though this experiment may not have been precise enough to identify differences in Re_{cr} between blood and water–glycerin.

Limitations. The vibration upstream of the stenosis in the rigid entrance pipe was measured once using LDV to ensure that the pump was not transmitting vibration in the circuit. The vibration level did not increase, meaning the increase in vibration observed in the latex is not a result of environmental noise (such as the pump) but is likely due to transitional flow. Since the system could not control the flowrate and temperature within the tight specification limits for extended durations, it was prudent to minimize measurement durations. Measurements of the WVV of the latex tube were conducted for as long as 12 s. It was found that

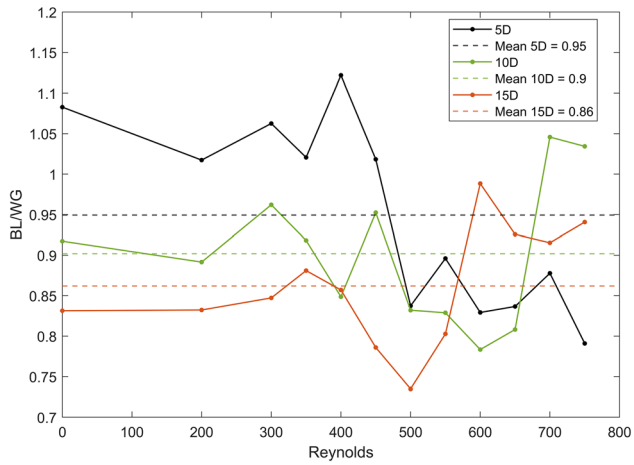

Fig. 8 Wall vibration velocity (WVV) RMS ratio of blood (BL) to water–glycerin (WG) for positions 5D, 10D, and 15D

measurements with a three seconds duration yielded similar results to those of twelve seconds, and as a result, this experiment limited the WVV to three seconds period.

For most cases, the AS peak frequency was 15–20 Hz for blood and water–glycerin (Figs. 5 and 6). Some spurious peaks were also found around 120 Hz and considered an artifact associated with temporary environmental disturbances. These disturbances were only found in position 5D for water–glycerin and lower Reynolds number (below 500). The dominant frequencies of measurements did not match the in vivo dominant frequencies found by Loth et al. and Lee et al., which were ~300 Hz and 100–250 Hz, respectively [9,10]. The disparity in frequency is obviously due to the different material properties of the pipe and the mean pressure within the tube. We did not try to match the in vivo frequency due to the convenience of the material availability and installation. Also, the primary goal was to compare the transition to turbulence between blood and water–glycerin under the assumption of a compliant wall and investigate how that would affect the delay in transition to turbulence previously found by Biswas et al. and Costa et al. Also, the steady flow condition may exacerbate the non-Newtonian effects. Ballyk et al. results showed that non-Newtonian blood rheology has a significant effect on steady flow wall shear stresses, but no significant effect on unsteady flow wall shear stresses [16].

Previous experiments found that the maximum experiment duration was limited to roughly two hours, after which point blood clots were known to form [3,7]. Since the maximum time allowed for blood inside the system was roughly two hours without clotting, only three positions and 12 Reynolds numbers were analyzed in this experiment. This time included removing air and bubbles from the system when inserting blood, temperature stabilization to 36.5–37.5 °C, density measurement, calibration of flowmeter, measurement at the three positions with vibrometer, and removal of fluid from the system. It was important to ensure that there were no bubbles in the system before experiments and calibration, which can be a source of error in the measurement. If more time were available, additional positions could be analyzed, a decrease in the Reynolds number increment or repeated studies could have been performed.

As with previous experiments by our group [3,7], Re_{cr} is sensitive to the measured fluid viscosity value; therefore, errors in the measurement of viscosity will result in errors in the Re_{cr}. Using a viscosity standard, the error of the rheometer was $< 3\%$. Thus, we can expect the measured values of whole blood and water–glycerin viscosity to be accurate for higher shear rates. There was some variability in the viscosity of the whole blood samples obtained from the slaughterhouse (standard deviation of viscosity at 1000 s^{-1} was 0.17, and density was 0.018). To prevent blood from clotting during the collection process, 20 ml (out of the total 100 ml) of anticoagulant was added early to the bucket for each aliquot of blood (i.e., 80 ml for the four aliquots). However, the slaughterhouse staff was unable to control the volume of blood collected in the receptacles with precision. Thus, the ratio of sodium citrate to blood might be slightly different each time. However, since we are using a nondimensional variable (Reynolds number) to represent each flow condition, the ratio differences of sodium citrate between samples are not believed to affect the results.

Finally, there is the possibility of even with long enough entrance length and using a turbulator mixer, small differences in flow perturbations may manifest in the inlet. However, based on previous studies, we know that the flow is laminar upstream of the stenosis from $Re < 1000$, and thus we do not believe small perturbations would manifest themselves between blood and WG. The FDA Nozzle study from Haley et al. showed that transition could be affected by slight perturbations, but here there should have been no systematic difference between the Newtonian and blood experiments that would make one noisier than the other [17].

Conclusions

Whole blood has a similar WVV during the transition to turbulence as the Newtonian fluid within a flexible tube downstream using a 5% eccentric stenosis with a 75% area reduction under steady flow conditions. No delay was detectible in the transition to turbulence for blood compared to water–glycerin. Blood was found to have a slightly smaller average WVV RMS compared to water–glycerin. This could be caused by the effect of the shear-thinning of blood or the effect of the density difference of the fluids. Since the rheological properties of blood did not affect the delay in transition to turbulence, this study suggests that a Newtonian assumption may be reasonable in blood flow simulations with compliant vessels where wall vibration is the parameter of interest near the transition to turbulence. This study is important to give some insights about the vibration level near the transition to turbulence downstream of a stenosis geometry, which is nontrivial vascular geometry associated with vascular diseases. Further research using a more direct measurement of fluid velocity fluctuations is required to fully understand the impact of flexible walls on the transition to turbulence for whole blood. It is also still necessary to understand the influence of vessel–tissue interaction as well as pulsatile flow in the transition to turbulence downstream of a stenosis for a flexible tube.

Acknowledgment

The authors acknowledge the support of Dale Ertley for manufacturing the stenosis model used in this study and the University of Akron.

Nomenclature

AS = amplitude spectrum
D = diameter
Re_{cr} = critical Reynolds number
RMS = root mean squared
TKE = turbulent kinetic energy
WVV = wall vibration velocity

References

[1] Baskurt, O., and Meiselman, H., 2003, "Blood Rheology and Hemodynamics," Semin. Thromb. Hemostasis, **29**(5), pp. 435–450.
[2] Nader, E., Skinner, S. C., Romana, M., Fort, R., Lemonne, N., Guillot, N., Gauthier, A., et alet al., 2019, "Blood Rheology: Key Parameters, Impact on Blood Flow, Role in Sickle Cell Disease and Effects of Exercise," Front. Physiol., **10**, pp. 1–14.
[3] Biswas, D., Casey, D. M., Crowder, D. C., Steinman, D. A., Yun, Y. H., and Loth, F., 2016, "Characterization of Transition to Turbulence for Blood in a Straight Pipe Under Steady Flow Conditions," ASME J. Biomech. Eng., **138**(7), p. 071001.
[4] Ahmed, S. A., and Giddens, D. P., 1983, "Velocity Measurements in Steady Flow Through Axisymmetric Stenoses at Moderate Reynolds Numbers," J. Biomech., **16**(7), pp. 505–516.
[5] Varghese, S., Frankel, S., and Fischer, P., 2007, "Direct Numerical Simulation of Stenotic Flows, Part 1: Steady Flow," J. Fluid Mech., **582**, pp. 253–280.
[6] Khan, M. O., Valen-Sendstad, K., and Steinman, D., 2019, "Direct Numerical Simulation of Laminar-Turbulent Transition in a Non-Axisymmetric Stenosis Model for Newtonian vs. Shear-Thinning Non-Newtonian Rheologies," Flow, Turbul. Combust., **102**(1), pp. 43–72.
[7] Costa, R. P., Nwotchouang, S. T. B., Yao, J., Biswas, D., Casey, D., McKenzie, R., Steinman, D. A., and Loth, F., 2022, "Transition to Turbulence Downstream of a Stenosis for Whole Blood and a Newtonian Analog Under Steady Flow Conditions," ASME J. Biomech. Eng., **144**(3), p. 031008.
[8] Gad-el-Hak, M., 2002, "Compliant Coatings for Drag Reduction," Prog. Aerosp. Sci., **38**(1), pp. 77–99.
[9] Lee, S., Fischer, P., Loth, F., Royston, T., Grogan, J. K., and Bassiouny, H. S., 2005, "Flow-Induced Vein-Wall Vibration in an Arteriovenous Graft," J. Fluids Struct., **20**(6), pp. 837–852.
[10] Loth, F., Fischer, P. F., Arslan, N., Bertram, C. D., Lee, S. E., Royston, T. J., Shaalan, W. E., and Bassiouny, H. S., 2003, "Transitional Flow at the Venous Anastomosis of an Arteriovenous Graft: Potential Activation of the ERK1/2 Mechanotransduction Pathway," ASME J. Biomech. Eng., **125**(1), pp. 49–61.
[11] Fillinger, M., Reinitz, E. R., Schwartz, R., Resetarits, D. E., Paskanik, A., Bruch, D., and Bredenberg, C., 1990, "Graft Geometry and Venous Intimal-Medial Hyperplasia in Arteriovenous Loop Grafts," J. Vasc. Surg., **11**(4), pp. 556–566.

[12] Kirkeeide, R., Young, D., and Cholvin, N. R., 1977, "Wall Vibrations Induced by Flow Through Simulated Stenosis in Models and Arteries," J. Biomech., **10**(7), pp. 431–441.
[13] Whitcomb, J. E., Amini, R., Simha, N. K., and Barocas, V. H., 2011, "Anterior-Posterior Asymmetry in Iris Mechanics Measured by Indentation," Exp. Eye Res. **93**(4), pp. 475–481.
[14] Hayes, W. C., Keer, L. M., Herrmann, G., and Mockros, L. F., 1972, "A Mathematical Analysis for Indentation Tests of Articular Cartilage," J. Biomech., **5**(5), pp. 541–551.
[15] Bergersen, A. W., Mortensen, M., and Valen-Sendstad, K., 2019, "The FDA Nozzle Benchmark: 'in Theory There is No Difference Between Theory and Practice, but in Practice There Is'," Int. J. Numer. Methods Biomed. Eng., **35**(1), p. e3150.
[16] Ballyk, P. D., Steinman, D. A., and Ethier, C. R., 1994, "Simulation of non-Newtonian Blood Flow in an End-to-Side Anastomosis," Biorheology, **31**(5), pp. 565–586.
[17] Haley, A. L., Valen-Sendstad, K., and Steinman, D. A., 2021, "On Delayed Transition to Turbulence in an Eccentric Stenosis Model for Clean vs. noisy High-Fidelity CFD," J. Biomech., **125**, p. 110588.